Zn(II) Ions Substantially Perturb Cu(II) Ion Coordination in Amyloid-beta at Physiological pH

ARTICLE *in* THE JOURNAL OF PHYSICAL CHEMISTRY B · JULY 2013

Impact Factor: 3.3 · DOI: 10.1021/jp406067n · Source: PubMed

2 AUTHORS, INCLUDING:

Sunil Saxena
University of Mumbai
78 PUBLICATIONS **555** CITATIONS

SEE PROFILE

THE JOURNAL OF PHYSICAL CHEMISTRY B

Article

pubs.acs.org/JPCB

Zn(II) Ions Substantially Perturb Cu(II) Ion Coordination in Amyloid-β at Physiological pH

K. Ishara Silva and Sunil Saxena*

Department of Chemistry, University of Pittsburgh, Pittsburgh, Pennsylvania 15260, United States

Supporting Information

ABSTRACT: The interaction of Cu(II) and Zn(II) ions with amyloid-β (Aβ) plays an important role in the etiology of Alzheimer's disease. We describe the use of electron spin resonance (ESR) to measure metal-binding competition between Cu(II) and Zn(II) in amyloid-β at physiological pH. Continuous wave ESR measurements show that the affinity of Cu(II) toward Aβ(1−16) is significantly higher than that of Zn(II) at physiological pH. Importantly, of the two known Cu(II) coordination modes in Aβ, component I and component II, Zn(II) displaces Cu(II) only from component I. Our results indicate that at excess amounts of Zn(II) component II becomes the most dominant coordination mode. This observation is important as Aβ aggregates in the brain contain a high Zn(II) ion concentration. In order to determine details of the metal ion competition, electron spin echo envelope modulation experiments were carried out on Aβ variants that were systematically ^{15}N labeled. In the presence of Zn(II), most peptides use His 14 as an equatorial ligand to bind Cu(II) ions. Interestingly, Zn(II) ions completely substitute Cu(II) ions that are simultaneously coordinated to His 6 and His 13. Furthermore, in the presence of Zn(II), the proportion of Cu(II) ions that are simultaneously coordinated to His 13 and His 14 is increased. On the basis of our results we suggest that His 13 plays a critical role in modulating the morphology of Aβ aggregates.

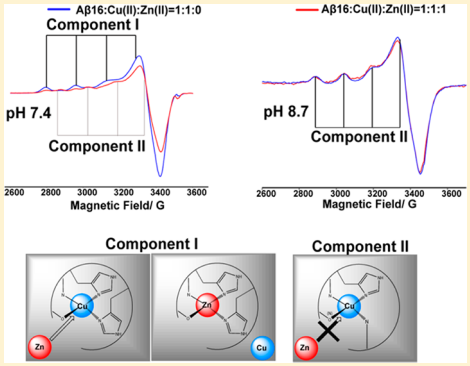

INTRODUCTION

Metal ion competition in biological systems is important for maintaining a proper ion balance, which in turn is critical for homeostasis.[1] Copper and zinc ions play critical roles in many biological pathways, including respiration, cell signaling, and electron transfer.[2−4] In the central nervous system, metal ion competition is critical as these metal ions are involved in a large variety of activities, including the development and maintenance of enzymatic activities, neurotransmission, etc.[5] Ionic imbalance in the central nervous system can lead to several neurological diseases, such as Alzheimer's disease, which is the most common cause of neurodegenerative dementia.[6−8]

Herein we examine the metal-binding competition in the Aβ peptide which is involved in Alzheimer's disease. Much research has been conducted to determine the role metal ions play in the etiology of Alzheimer's disease. Interestingly, micro-particle-induced X-ray emission microscopy measurements have shown that amyloid aggregates in brain tissues show abnormally high levels of Cu(II) and Zn(II).[9] Furthermore, these metal ions are colocalized within the Aβ deposits.[9] Several coordination modes have been proposed for these metal ions in Aβ on the basis of several spectroscopic techniques such as nuclear magnetic resonance (NMR), circular dichroism, X-ray absorption spectroscopy, electrospray-ionization mass spectroscopy, and Raman spectroscopy.[10−13] Most of these investigations were focused on single metal ion coordination in Aβ. In this work, we utilize electron spin resonance (ESR) in conjunction with isotopic labeling to establish the coordination environment of Cu(II) in the presence of Zn(II).

The higher concentration of these ions in amyloid plaques[9] raises the possibility that these metal ions might be involved in the plaque formation. Aβ peptide undergoes metal-induced oligomerization under physiological conditions.[14] It is important to note that the aggregated states of Aβ-Cu(II) and Aβ-Zn(II) are very different. Saxena and co-workers reported that Cu(II) induces mature fibril formation at sub-equimolar concentrations, while granular amorphous aggregates are observed at higher concentrations of Cu(II).[15] Zn(II) on the other hand forms more amorphous aggregates rather than fibrillar aggregates even at sub-equimolar concentrations.[16,17] It has been suggested that the different coordination modes of Cu(II) and Zn(II) ions in Aβ are related to the different morphologies and toxicities of aggregates.[18,19]

The Cu(II) ion coordination in Aβ(1−16) has been shown to be identical to that in the full length Aβ.[20−22] Continuous wave electron spin resonance (CW-ESR) spectroscopy has revealed that there are two major coordination modes in Aβ-Cu(II), known as component I and component II.[23−25] Component I is the major Cu(II) coordination mode at physiological pH, accounting for 65−75% of the overall coordination.[10,26] A number of experimental techniques have

Received: June 19, 2013
Revised: July 8, 2013
Published: July 10, 2013

   dx.doi.org/10.1021/jp406067n | J. Phys. Chem. B 2013, 117, 9386−9394

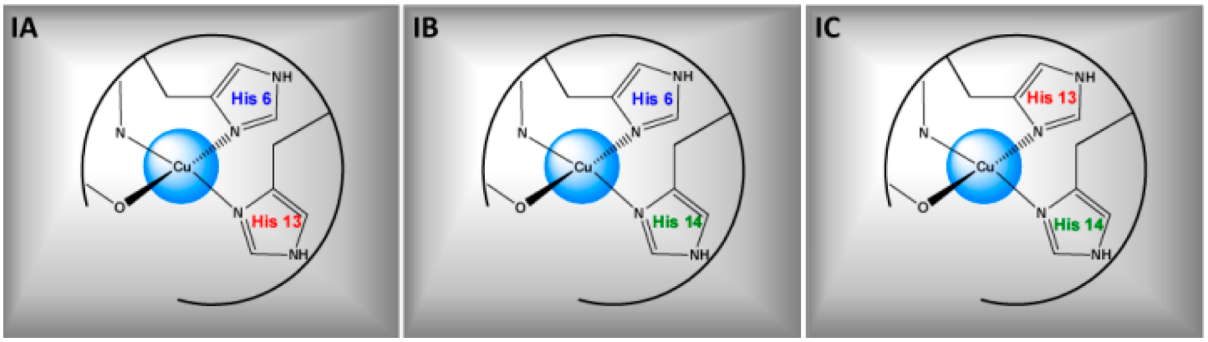

Figure 1. Three proposed subcomponents for component I in Cu(II) coordinated to Aβ peptide. In subcomponent IA, His 6 and 13 simultaneously coordinate the Cu(II) ion in the equatorial plane. Subcomponent IB Cu(II) coordinates His 6 and 14, while subcomponent IC coordination contains His 13 and 14.

revealed that the histidine residues in Aβ at positions 6, 13, and 14 are involved in the Cu(II) coordination.[10,12,13,25] Previous work done in our group using electron spin echo envelope modulation (ESEEM) spectroscopy and hyperfine sublevel correlation (HYSCORE) showed that all three histidine residues in Aβ(1−16) are involved in the coordination of Cu(II).[27] In component I, Cu(II) is thought to be coordinated to two out of three histidine residues present in Aβ at positions 6, 13, and 14. Depending on which histidine residues are coordinated to Cu(II), two possible coordination modes for Cu(II) component I were proposed at pH 6.0.[24] Component IA contains simultaneous coordination of His 6 and His 13, while component IB contains His 6 and His 14 (Figure 1). At pH 6.0, the simultaneous coordination of Cu(II) by His 13 and His 14 is almost nonexistent. However, Shin et al. showed that simultaneous coordination of His 13 and His 14 is as important as His 6 and His 13 coordination at physiological pH.[26] Thus, a subcomponent IC, as shown in Figure 1, was introduced to account for the simultaneous His 13 and His 14 coordination. A recent investigation done in Aβ(1−40) fibrils using pulsed ESR revealed a bis-*cis*-His equatorial coordination geometry for Cu(II).[28] Also, this research proposed a structure in which Cu(II) is coordinated to His 6/His 13 and His 6/His 14 alternatively along the fibrillar axis on opposite sides of the β-sheet structure.[28] The other two equatorial ligands for Cu(II) component I are believed to be the N-terminus[21,24,25] and the carbonyl oxygen from Asp 1.[24]

The metal-binding site for Zn(II) ion lies in the N-terminal hydrophilic region of Aβ(1−16), as is the case for Cu(II).[29,30] It is believed that all three histidine residues are involved in the coordination of Zn(II) in Aβ(1−16).[30−34] Classically, Zn(II) coordination involves four to six ligands. The identities of other ligands are still controversial. The Aβ ligands proposed in binding Zn(II) in addition to the three histidine residues are the N-terminal amine from Asp 1, the Glu 11 carboxylate side chain, the deprotonated amide of the Arg 5 backbone, and Tyr 10.[10]

The Cu(II) coordination in Aβ(1−16) is heterogeneous and involves all three histidine residues in different coordination modes. Given the coexistence of Cu(II) and Zn(II) in amyloid plaques, it is critical to study the Cu(II) coordination in the presence of Zn(II). This represents a better depiction of the *in vivo* environment. We used CW-ESR spectroscopy in conjunction with simulations to determine how Zn(II) competes with Cu(II) for Aβ(1−16) coordination at physiological pH. These results show that the overall affinity of Cu(II) toward Aβ(1−16) is higher than that of Zn(II). Importantly, only component I of Cu(II) was substituted by Zn(II). ESEEM experiments were performed at low magnetic field strength (2800 G), at which only component I of Cu(II) coordination is present. Single-labeled and double-labeled peptides containing one and two ^{15}N isotopically labeled histidine residues were used to obtain detailed information on the role of each histidine residue in Cu(II) coordination. In the presence of an equimolar amount of Zn(II), the ESEEM results suggest that approximately half of the peptides in the ensemble use His 14 as an equatorial ligand for Cu(II) coordination in component I. Furthermore, the proportion of subcomponent IC was increased in the presence of Zn(II). The atomic force microscopy (AFM) results obtained using Aβ(1−40) show that amorphous aggregates are prevalent in the presence of both Zn(II) and Cu(II).

EXPERIMENTAL SECTION

Peptide Synthesis and Cu(II)/Zn(II) Complex Preparation. Isotopically enriched [G-^{15}N]-N$_\alpha$-Fmoc-N$_\tau$-trityl-L-histidine, in which all nitrogen atoms are ^{15}N-enriched, was purchased from Cambridge Isotope Laboratory (Andover, MA). Three different variants of amyloid-β(1−16) (DAEFRHDSGYEVHHQK) containing an ^{15}N-enriched histidine at position 6, 13, or 14 were synthesized at the Molecular Medicine Institute, University of Pittsburgh, using standard fluorenylmethoxycarbonyl chemistry.[35,36] Double-labeled peptides containing two ^{15}N-enriched histidine residues were synthesized in the same manner. All the labeled amyloid-β(1−16) variants were purified by high-performance liquid chromatography and characterized by mass spectroscopy. Nonlabeled amyloid-β(1−16) peptide was purchased from rPeptide (Bogart, GA). Isotopically enriched (98.6%) $^{63}CuCl_2$ was purchased from Cambridge Isotope Laboratory, and anhydrous $ZnCl_2$ powder (≥99.995% metal basis) was purchased from Sigma-Aldrich Co. (St. Louis, MO). The enriched isotope was used to minimize inhomogeneous broadening of the Cu(II) ESR spectra. *N*-Ethylmorpholine (NEM) was purchased from Sigma-Aldrich Co.

The 2.5 mM solutions of peptides were prepared in 100 mM NEM buffer (pK_a = 7.8) at pH 7.4 in 50% (v/v) glycerol and appropriate amounts of hydrochloric acid. Cu(II) and Zn(II) stock solutions at 10 mM were prepared in NEM buffer. Appropriate amounts of stock solutions of Cu(II) and Zn(II) were added to a tube. Then the peptide was added to the tube containing Cu(II) and Zn(II) to make sure the peptide coordinates with both the metal ions simultaneously. The final peptide concentration of the ternary complexes was 1.25 mM.

dx.doi.org/10.1021/jp406067n | J. Phys. Chem. B 2013, 117, 9386−9394

For all ESEEM experiments equivalent amounts of Cu(II) and Zn(II) were added (peptide:Cu(II):Zn(II) = 1:1:1). For CW experiments the metal ion concentrations were changed to provide the desired ratios. Samples of double-isotopic labeled peptide were prepared following the same procedure used for the single-isotopic labeled peptides.

Electron Spin Resonance Spectroscopy. A 200 μL aliquot of the sample was transferred into a quartz tube with an inner diameter of 3 mm. Electron spin resonance experiments were performed on either a Bruker ElexSys E580 or a Bruker ElexSys E680 X-band FT/CW spectrometer equipped with a Bruker ER4118X-MD5 or EN4118X-MD4 resonator, respectively. The temperature was controlled using an Oxford ITC503 temperature controller and an Oxford CF935 dynamic continuous flow cryostat connected to an Oxford LLT 650 low-loss transfer tube. All samples were frozen quickly by immersion in liquid nitrogen. Then the samples were inserted into the sample cavity which was precooled to the desired temperature (20 or 80 K).

Continuous-wave ESR experiments were carried out on sample solutions at 80 K with a microwave frequency of approximately 9.69 GHz. The magnetic field was swept from 2600 to 3600 G for 1024 data points. A time constant of 40.96 ms, a conversion time of 81.92 ms, a modulation amplitude of 4 G, a modulation frequency of 100 kHz, and a microwave power of 0.1993 mW were the other instrument parameters used for the CW experiment. The experimentally obtained spectra were compared with simulations using Bruker Simfonia.

Three-pulse ESEEM experiments were performed on the sample solutions at 20 K, using a $\pi/2-\tau-\pi/2-T-\pi/2-$echo pulse sequence with a $\pi/2$ pulse width of 16 ns. The first pulse separation, τ, was set at 144 ns, and the second pulse separation, T, was varied from 288 ns with a step size of 16 ns with the magnetic field strength fixed at 2800 G. Component I of the Cu(II)-Aβ(1−16) complex is almost exclusively observed at this magnetic field at physiological pH. Four-step phase cycling was employed to eliminate unwanted echoes.[37,38] The raw data were phase corrected, and the real part was selected. After the baseline correction, the data were fast Fourier transformed. Then the final spectra were obtained as the magnitude of the Fourier transforms.

Four-pulse HYSCORE experiments were carried out at 20 K with a $\pi/2-\tau-\pi/2-t_1-\pi-t_2-\ \pi/2-\tau-$echo pulse sequence with $\pi/2$ and π pulse lengths of 16 and 32 ns, respectively. The first pulse separation, τ, was set at 144 ns, and both the second (t_1) and third (t_2) pulse separations were varied with a step size of 16 ns and 100 shots per points. The final data consisted of 256 data points in both t_1 and t_2. The magnetic field was fixed at 3360 G, where the echo intensity is a maximum. Four-step phase cycling was employed to eliminate unwanted signals. The real parts of the collected two-dimensional data were baseline corrected and zero filled to 1024 points in both dimensions. After the two-dimensional Fourier transformation was performed, the final spectra were obtained as contour plots of the magnitude of the Fourier transforms.

ESEEM Data Analysis. For systems where Cu(II) is coordinated to ^{14}N, the ESEEM spectrum contains three characteristic peaks between 0 and 2 MHz.[39−43] When the exact cancellation condition is fulfilled, these three ESEEM frequencies correspond to υ_0, υ_-, and υ_+ for the nuclear quadrupole interaction (NQI) transitions.

$$\nu_0 = \frac{e^2qQ\eta}{2h};\ \nu_- = \frac{e^2qQ(3-\eta)}{4h};\ \nu_+ = \frac{e^2qQ(3+\eta)}{4h} \tag{1}$$

In the equations above, e is the electron charge, q the z-component of the electric field gradient across the nucleus, Q the ^{14}N nuclear quadrupole moment, η the asymmetry parameter, and h Planck's constant.

Apart from these three NQI peaks there is a broad peak around 3.8 MHz, which is attributed to a double quantum (DQ) transition.[39−43] The double quantum transition frequency is given by[44]

$$\nu_{DQ} = 2\left[\left(\nu_I + \frac{A}{2}^2\right) + \left(\frac{B}{2}\right)^2 + \left(\frac{e^2qQ}{4h}\right)(3+\eta^2)\right]^{\frac{1}{2}} \tag{2}$$

where ν_{DQ} is the double quantum transition frequency and ν_I is the Larmor frequency of ^{14}N; A and B are the secular and the pseudo-secular part of the hyperfine interaction, respectively.

In this work we compare the ESEEM signals of wild-type Aβ(1−16) with those of ^{15}N-labeled Aβ(1−16) peptides. Upon ^{15}N substitution, the modulation depths of the signals due to ^{14}N nuclei will decrease in ESEEM. This decrease is because the single quantum transition of ^{15}N nuclei does not substantially contribute to the ESEEM signal.[43,45−49] In our approach, the ^{14}N-ESEEM signal is normalized by the ^{1}H-ESEEM signal as the ^{1}H-ESEEM modulation depth is not affected by a replacement of ^{14}N with ^{15}N. The decrease in the relative modulation depth of the ^{14}N nuclear transition frequency can be calculated by comparing the relative integrated intensity of the ^{15}N-labeled peptide with the nonlabeled peptide. For a single ^{14}N nucleus coupled to an electron spin system, this decrease in modulation depth is[26]

$$\frac{K^{\alpha}_{14(\text{labeled})}/K_{1(\text{labeled})}}{K^{\alpha}_{14(\text{nonlabeled})}/K_{1(\text{nonlabeled})}} = \frac{(1-f)[2-(K^{\alpha}_{14}+K^{\beta}_{14})]}{2-(1-f)(K^{\alpha}_{14}+K^{\beta}_{14})} \tag{3}$$

where K is the modulation depth and f is the fraction of ^{14}N nuclei that have been replaced. Subscripts 14 and 1 denote the ^{14}N spin and ^{1}H spin, respectively. Superscripts α and β represent the α and β spin manifolds of the electron spin, respectively. Shin and Saxena showed that this normalized ^{14}N modulation depth is a monotonic function of the fraction of ^{14}N that is replaced with ^{15}N.[26] It is evident that the decrease in the relative modulation depth of the ^{14}N nuclear transition frequency is greater than that in the fraction of ^{14}N. If K^{α}_{14} and K^{β}_{14} are much smaller than 1, the factor converges to $1-f$, which is the fraction of ^{14}N. For example, if the K^{α}_{14} and K^{β}_{14} values are approximately 0.15, eq 3 becomes

$$\frac{K_{14(\text{labeled})}/K_{1(\text{labeled})}}{K_{14(\text{nonlabeled})}/K_{1(\text{nonlabeled})}} = \frac{1.70(1-f)}{1.70+0.30f} \tag{4}$$

In the case of a 33% replacement of ^{14}N with ^{15}N, the ratio $F(m^{15}\text{N}/0^{15}\text{N})$ is approximately 0.63, which indicates that the relative modulation depth of the ^{14}N transition frequency decreases by 37%, just 4% greater than the value expected based on the the fraction of replacement.

However, it is difficult to obtain modulation depths as many components are overlaid in the ESEEM time domain curve. Shin and Saxena showed that the integrated intensity can be used to account for the decrease in the modulation depth upon

dx.doi.org/10.1021/jp406067n | J. Phys. Chem. B 2013, 117, 9386−9394

^{15}N labeling in the ^{14}N-ESEEM signal.[26] In the frequency domain the ^{1}H signal is well-separated from the signal produced by ^{14}N, so it is possible to integrate each separately. The ^{14}N-ESEEM integrated intensity is obtained by integrating between 0 and 8 MHz, and for the ^{1}H-ESEEM, the integration is done between 10 and 14 MHz. Thus, relative integrated intensities can be used to calculate the fraction of ^{14}N nuclei coordinated to Cu(II). Detailed equations for multiple histidine coordination are provided in ref 22.

RESULTS

Zn(II) Competes with Cu(II) for Aβ(1−16) Coordination. Continuous-wave ESR experiments were carried out on the equimolar mixture of Cu(II) and Aβ(1−16) in the presence and absence of Zn(II) in 100 mM NEM (pH 7.4) buffer. These experiments were performed to demonstrate the binding competition between Cu(II) and Zn(II) for Aβ(1−16) coordination. As Zn(II) is a diamagnetic ESR silent species, the change in the Cu(II) signal is used to investigate the effects of Zn(II) in the system. At the physiological pH in NEM buffer, free Cu(II) precipitates and does not contribute to the signal.[23] Figure 2 shows the experimentally obtained CW-ESR spectra in the presence and absence of Zn(II). In the presence of 1 equiv of Zn(II), the intensity of the ESR signal decreased as shown in Figure 2. Quantitatively the double-integrated intensity was reduced by ∼25%. Upon the addition of 4 equiv of Zn(II), the double-integrated signal intensity of Cu(II) was decreased by ∼40%. The decrease in the double-integrated intensity of the Cu(II) signal clearly illustrates the fact that Zn(II) competes with Cu(II) for Aβ(1−16) coordination. To understand how the Cu(II) signal intensity changes with the increase in Zn(II) concentration, further CW experiments were carried out. The ratios of Aβ(1−16) and Cu(II) were kept constant, and the Zn(II) ratio was changed from 0 to 10 in these experiments. The double-integrated intensity of these CW spectra was calculated to elucidate the amount of Cu(II) bound to the peptide at different Zn(II) ratios (Supporting Information, Figure S1). The amount of bound Cu(II) remains approximately constant after the addition of 4 equiv of Zn(II) to the mixture. Approximately 60% of the initially added Cu(II) is still bound to Aβ(1−16) even at large excess concentrations of Zn(II) under conditions where both metal ions compete simultaneously for peptide coordination.

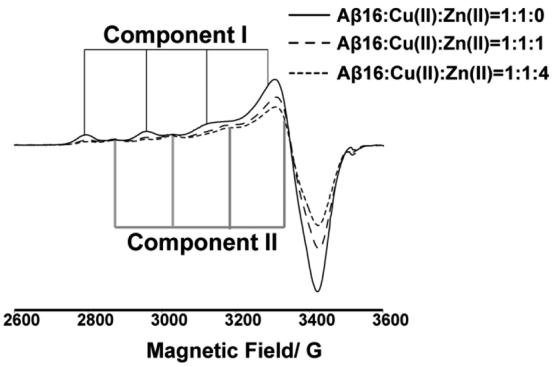

Figure 2. CW-ESR spectra illustrating the reduction of Cu(II) intensity in the presence of Zn(II) when coordinated to Aβ(1−16) peptide at physiological pH. At equimolar amounts, Zn(II) reduces the double-integrated intensity of the Cu(II) signal by ∼25% with respect to the Zn(II)-absent spectra, and at 4 equiv of Zn(II), the signal intensity is reduced by ∼40%.

Zn(II) Competes Only with Component I of Cu(II) at Physiological pH. The Aβ(1−16)-Cu(II) CW spectrum contains two clear components at physiological pH (Figure 2). Component I, which is the major component of Cu(II) coordination at physiological pH, has $g_{\|}$ and $A_{\|}$ values of 2.26 ± 0.005 and 170 ± 1 G, respectively. These ESR parameters are consistent with a type II Cu(II) center, coordinated to three nitrogen ligands and one oxygen ligand in the equatorial plane.[50] Likewise, the $g_{\|}$ and $A_{\|}$ values of 2.23 ± 0.005 and 156 ± 1 G, respectively, of component II are consistent with coordination of either three nitrogen ligands and one oxygen ligand or four nitrogen ligands.[50]

A close inspection of CW-ESR spectra of Aβ(1−16)-Cu(II) and Aβ(1−16)-Cu(II)/Zn(II) showed an interesting pattern. Figure 3a shows the CW-ESR spectra of Aβ(1−16)-Cu(II) and Aβ(1−16)-Cu(II)/Zn(II) complexes at pH 7.4. Interestingly, in the presence of Zn(II) the intensity of only component I was decreased. The intensity of component II remains very similar in both the presence and the absence of Zn(II). Spectral simulations were performed to quantify the proportion of each component in the Aβ(1−16)-Cu(II) complex. ESR parameters

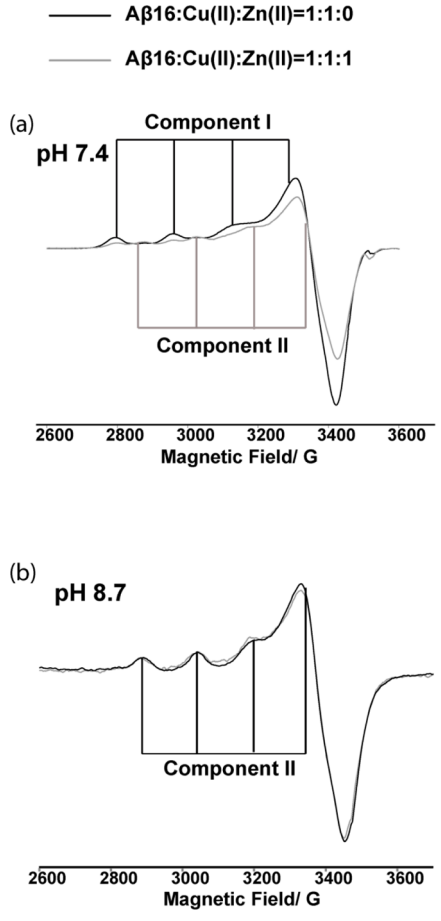

Figure 3. (a) Overlay of CW-ESR spectra of Aβ(1−16)-Cu(II) equimolar binary complex (black) and Aβ(1−16)-Cu(II)/Zn(II) equimolar ternary complex (gray) at pH 7.4 and (b) at pH 8.7. At pH 8.7, only component II of Cu(II) binding is present. Interestingly, the double-integrated intensity of the spectra remains almost the same, suggesting Zn(II) cannot compete with Cu(II) for component II coordination.

dx.doi.org/10.1021/jp406067n | J. Phys. Chem. B 2013, 117, 9386−9394

used for the CW simulations are tabulated in the Supporting Information, Table S2. An overlay of experimental and simulation results is shown in the Supporting Information, Figure S2. In the absence of Zn(II), component I was the major component and accounts for ∼65% of the overall signal. However, in the Aβ(1−16)-Cu(II)/Zn(II) equimolar complex the amount of component I is ∼50%. At a 4-fold excess of Zn(II), the proportion of component I is ∼35%. To confirm the selective substitution of Cu(II) by Zn(II), experiments were repeated at pH 8.7. At this pH, only component II of Cu(II) binding is present. The double-integrated intensity of the Cu(II) signal in the presence and absence of 1 equiv of Zn(II) remained approximately the same, as shown in Figure 3b, indicating that Zn(II) was unable to displace Cu(II) from component II.

Contribution of Each Histidine Residue for Component I in Aβ(1−16)-Cu(II)/Zn(II) Complex. As discussed earlier, all three histidine residues are involved in the Cu(II) coordination at physiological pH[24,25,27] and component I consists of three subcomponents (Figure 1).[26] Our CW results show that Zn(II) competes only with Cu(II) for component I coordination. Thus, it is of interest to discover which subcomponents of component I compete with Zn(II) for Aβ(1−16) coordination by evaluating the contribution of each histidine residue to the Cu(II) coordination in component I. Experiments are carried out at a magnetic field strength of 2800 G, where the contribution from component II is negligible.

Figure 4 shows the ESEEM spectrum of unlabeled Aβ(1−16) peptide coordinated to Cu(II) and Zn(II) at physiological pH

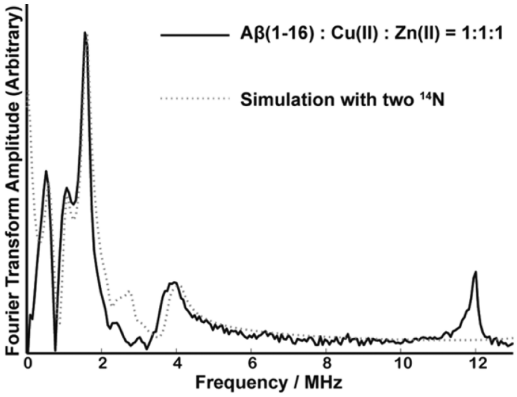

Figure 4. Experimentally obtained and simulated three-pulse ESEEM spectra of the nonlabeled Aβ(1−16) peptide mixed with equimolar amounts of Cu(II) and Zn(II) at 2800 G and pH 7.4.

and 2800 G. The spectrum contains three peaks around 0.55, 1.01, and 1.54 MHz. The nuclear quadrupole parameters, e^2qQ/h and η, are determined to be 1.70 ± 0.03 MHz and 0.65 ± 0.02, respectively. These numbers are comparable to those for Cu(II) histidine complexes.[39−42] The broad peak around 3.8 MHz is due to a double quantum (DQ) transition of the remote nitrogen of the imidazole.[51,52] As two histidine residues are likely simultaneously coordinated to Cu(II) on the equatorial plane, two simultaneous histidine coordinations are assumed to yield the best fit for ESEEM simulation (Figure 4). Apart from the peaks arising from ^{14}N, there is another peak around 11.9 MHz which is similar to the ^{1}H Larmor frequency at 2800 G. This peak is a result of hydrogen atom(s) weakly interacting with the electron spin of Cu(II).

Next, we analyzed the three-pulse ESEEM spectra obtained for three singly labeled Aβ(1−16) peptide variants. The spectra are shown in Figure 5. In these peptides, a single histidine at

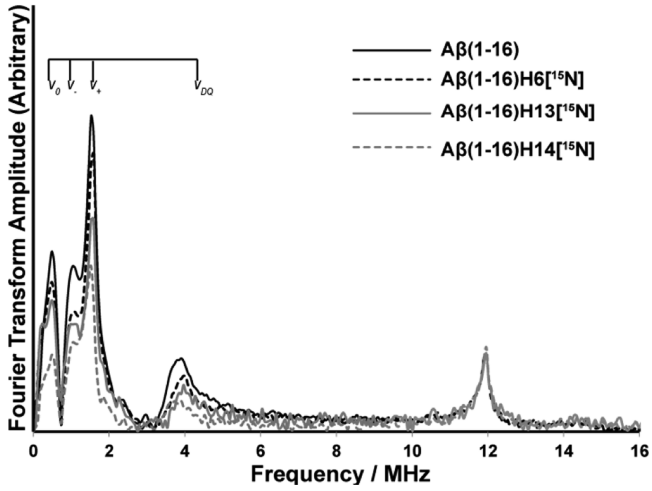

Figure 5. Three-pulse ESEEM spectra of the nonlabeled and single-^{15}N-labeled Aβ(1−16) variants mixed with equimolar amounts of Cu(II) and Zn(II) at 2800 G and pH 7.4 (peptide:Cu(II):Zn(II) = 1:1:1). The decrease in intensity below 8 MHz in ^{15}N-labeled Aβ(1−16) variants gives the contribution of each histidine residue for component I in the Aβ(1−16)-Cu(II)/Zn(II) complex. Aβ(1−16)H6[^{15}N], Aβ(1−16)H13[^{15}N], and Aβ(1−16)H14[^{15}N] denote peptides in which His 6, His 13, and His 14 are labeled with ^{15}N, respectively.

either His 6, His 13, or His 14 is isotopically labeled with ^{15}N. All these Aβ(1−16) variants were mixed with equivalent amounts of Cu(II) and Zn(II) at pH 7.4. The four spectra have similar line shapes and peak positions in the ^{14}N-ESEEM region. The similarity in the peak shapes implies that the ESEEM active ^{14}N of each histidine residue has almost the same nuclear transition frequencies.[42] In ESEEM experiments, the ^{14}N-ESEEM intensity is related to the number of ^{14}N histidine residues coordinated to Cu(II) (see Experimental Section). The single-quantum transition of ^{15}N, a nucleus with a spin of 1/2, contributes minimally (∼2%) toward the ESEEM signal.[43,48] Hence, when a ^{14}N nucleus is replaced with a ^{15}N the ESEEM signal intensity will decrease.

The three-pulse ESEEM spectra of three single-labeled peptides and the wild type were normalized using their ^{1}H-ESEEM intensities at or around 11.9 MHz. Then the ESEEM spectra were integrated between 0 and 8 MHz and compared between the wild-type and the ^{15}N-labeled peptides (see Experimental Section). As Figure 5 illustrates, the ^{15}N-labeled variants have lower intensities in the ^{14}N region below 8 MHz. At physiological pH, the normalized ^{14}N-ESEEM intensity of His 14-labeled peptide decreased by approximately 50% compared to that of the unlabeled ternary complex (Aβ(1−16)H14[^{15}N] in Figure 5). The decrease in ^{14}N-ESEEM intensity indicates that ∼50% of the peptides in the ensemble use His 14 as an equatorial ligand in Cu(II) coordination. The reductions of ^{14}N-ESEEM intensity for His 6- and His 13-labeled samples were ∼20% (Aβ(1−16)H6[^{15}N] in Figure 5) and 30% (Aβ(1−16)H13[^{15}N] in Figure 5), respectively. These values suggest that ∼20% and ∼30% of the peptides in the mixture equatorially coordinate to Cu(II) through His 6 and His 13, respectively. Hence, His 14 becomes the most

dx.doi.org/10.1021/jp406067n | J. Phys. Chem. B 2013, 117, 9386−9394

significant equatorially coordinated histidine ligand in Cu(II) binding (~50%) in component I. In the Aβ(1−16)-Cu(II) binary complex, both His 6 and His 14 were equally important in Cu(II) binding, each accounting for ~40%.[26] Thus, the Cu(II) coordination environment is rearranged in the presence of Zn(II).

The same set of experiments was carried out using three double-labeled Aβ(1−16) variants. In these double-labeled peptides, two out of three histidine residues in Aβ(1−16) are isotopically labeled with ^{15}N. As two of the three histidine residues are labeled, ^{14}N-ESEEM signal intensity results only from the nonlabeled histidine. This provides a direct methodology for determining the extent to which each of these residues is involved in the ternary complex. All the experiments were carried out at 2800 G, where only component I is present.

Despite a low signal-to-noise ratio, because of the fact that only one histidine is responsible for the ^{14}N-ESEEM signal, we were able to do the analysis with extensive signal averaging. As shown in Figure 6, as expected, His 14 was the highest-

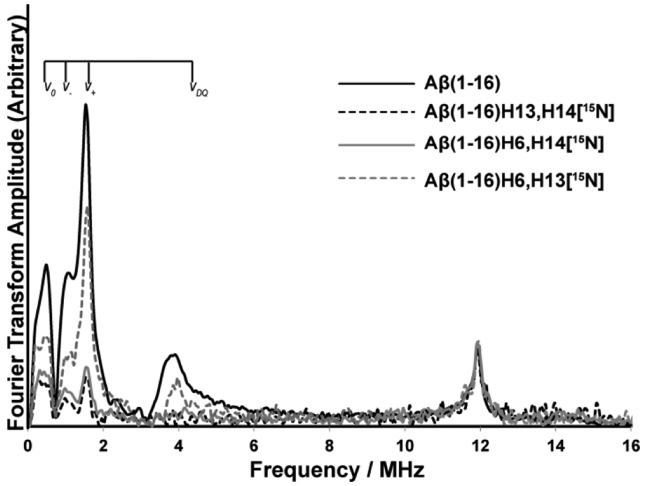

Figure 6. Three-pulse ESEEM spectra of the nonlabeled and double-^{15}N-labeled Aβ(1−16) variants mixed with equimolar amounts of Cu(II) and Zn(II) at 2800 G and pH 7.4 (peptide:Cu(II):Zn(II) = 1:1:1). The integrated area between 0 and 8 MHz gives the contribution of the nonlabeled histidine residue in double-labeled Aβ(1−16) variants for component I in the Aβ(1−16)-Cu(II)/Zn(II) complex. Aβ(1−16)H13,14[^{15}N], Aβ(1−16)H6,14[^{15}N], and Aβ(1−16)H6,13[^{15}N] denote peptides where His 13 and His 14, His 6 and His 14, and His 6 and His 13 are labeled with ^{15}N, respectively.

contributing histidine ligand in Cu(II) coordination in the ternary complex. The ESEEM signal intensity of His 6- and His 13-labeled peptide (in which only His 14 gives rise to the signal) is approximately 50% of that of the nonlabeled peptide (Aβ(1−16)H6,13[^{15}N] in Figure 6). This signal intensity indicates that ~50% of the peptides in the mixture use His 14 as an equatorial ligand. The ESEEM signal intensities of Aβ(1−16)H6,13[^{15}N] (His 6 nonlabeled) and Aβ(1−16)H6,13[^{15}N] (His 13 nonlabeled) were ~20% and ~30%, respectively. Hence, the percentages of each histidine residue involved as an equatorial ligand in Cu(II), obtained from both single- and double-labeled peptides, were similar. The integrated intensities of each spectrum and the relative contributions from each histidine residue toward the ^{14}N-ESEEM signal are tabulated in the Supporting Information, Tables S3 and S4.

The integrated intensity of the DQ peak depends on the number of ^{14}N-ESEEM active histidine residues.[40] Hence, the double quantum signal was weak in the double-labeled peptides as only one ^{14}N-ESEEM active histidine residue is present. Comparison between the single- and double-labeled peptide showed that the DQ integrated intensity is greater in the single-labeled peptide. If there is just single-histidine coordination, the DQ intensity would remain similar between the single- and double-labeled peptides. Therefore, the simultaneous coordination of two histidine residues in component I of the Aβ(1−16)-Cu(II)/Zn(II) ternary complex is preserved as it is in the Aβ(1−16)-Cu(II) binary complex.[24−26]

HYSCORE experiments were carried out in nonlabeled and labeled Aβ(1−16)-Cu(II)/Zn(II) at physiological pH and at the magnetic field of 3360 G. The spectra obtained showed the same frequency patterns as in the Cu(II) complex,[26,27] indicating that despite the presence of Zn(II), the coordination of Cu(II) remains essentially unchanged (Supporting Information, Figure S3). The primary difference between the two sets of spectra was that the intensities of correlation peaks were reduced as Zn(II) replaced approximately 25% of bound Cu(II) at equimolar amounts.

DISCUSSION

Selective Zn(II) Competition for Component I Cu(II) Coordination. Much work has been performed to determine the coordination environments and aggregate forms of Aβ in the presence of metal ions such as Cu(II) and Zn(II). However, multiple metal ion interactions in Aβ are not well-understood. The changes in Cu(II) coordination modes in the presence of Zn(II) in prion protein were examined using CW-ESR[53] and X-ray absorption spectroscopy (XAS).[54] These results in Aβ(1−16) show the usefulness of ESEEM to elucidate molecular level details of metal ion competition and coordination. These kinds of experiments are important as multiple metal ions coexist in an *in vivo* environment. Using CW-ESR and spectral simulations we established that Zn(II) competes only with component I at physiological pH. Our CW-ESR and simulations revealed that at excess amounts of Zn(II), component II becomes the most significant coordination mode. In brain tissues affected with Alzheimer's disease, the concentration of zinc is higher than that of copper.[9] Hence, it will be critical to understand the microscopic details of component II coordination.

Change in Component I Cu(II) Coordination in Aβ(1−16) in the Presence of Zn(II). The ESEEM results show that at physiological pH proportions of peptides coordinated through histidine residues in the equatorial plane are in the order His 14 > His 13 > His 6. These contributions are significantly different from the contributions reported for component I in the Cu(II)-Aβ(1−16) binary complex. Previous work done in our group reported that the order for the binary complex was His 14 ~ His 6 > His 13.[26] This is the first investigation reporting the contributions of each histidine residue in the Aβ(1−16)-Cu(II)/Zn(II) ternary complex. These results suggest the importance of His 14 in Cu(II) coordination in the presence of Zn(II).

Damante et al.,[55] in their work done using the Aβ(1−16)-polyethylene glycol ylated peptide, suggested that the addition of Zn(II) does not liberate Cu(II) ions but modifies the metal ion distribution in Aβ(1−16). In our findings, Zn(II) can partially substitute (~25%) bound Cu(II) from Aβ(1−16) at equimolar concentrations. Also, the present work adds critical

dx.doi.org/10.1021/jp406067n | J. Phys. Chem. B 2013, 117, 9386−9394

details regarding the redistribution of Cu(II). Using the proportions of each histidine residue involved in Aβ(1−16)-Cu(II), the proportion of peptides in each component was calculated (see Figure S4 in Supporting Information for more details).[26] Figure 7 shows the overall coordination environment

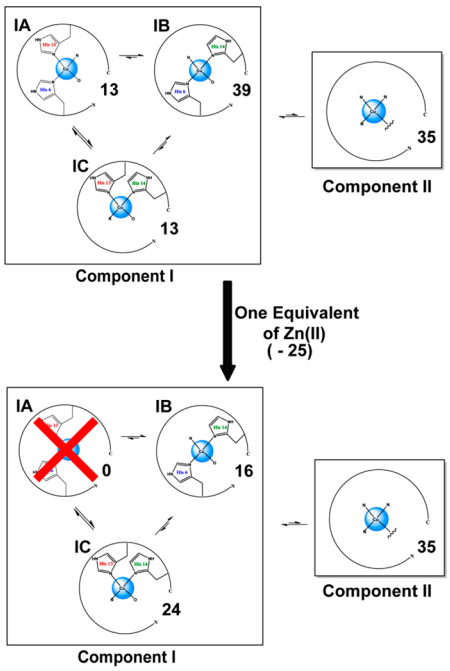

Figure 7. Overall population distribution of Cu(II)-binding modes in Aβ(1−16) in the presence and absence of Zn(II) at physiological pH. The proportion of subcomponent IC, which may inhibit the formation of ordered fibrillar forms, is increased. Subcomponent IA is no longer present in the presence of Zn(II), and the IB proportion is decreased.

of Cu(II) in Aβ(1−16) in the presence and absence of 1 equiv of Zn(II). Notably, all the Cu(II) ions in subcomponent IA, in which the metal ion is simultaneously coordinated to His 6 and His 13, are replaced by Zn(II). The proportion of Cu(II)-coordinated peptides in subcomponent IB is decreased, while the number of peptides in subcomponent IC is increased. These observations can be rationalized using the individual affinities of histidine residues toward Cu(II). The affinity of each histidine residue is in the order His 14 > His 13 ~ His 6.[26] This order would suggest Zn(II) is more likely to remove Cu(II) coordinated to His 6 and His 13 than it is to remove Cu(II) coordinated to His 14. Hence, Zn(II) is most likely to substitute Cu(II) in subcomponent IA.

Information on Cu(II) and Zn(II) coordination in Aβ will help establish the conformational preferences and structure of the N-terminus. This insight is crucial because current models of structure do not include any metal ions. Furthermore, these results are also likely to guide rational structure-based design of metal chelates as therapeutics for Alzheimer's disease.[56−58]

Physiological Importance of Simultaneous His 13 and His 14 Coordination. It is known that at greater than equimolar concentrations the proportion of amorphous aggregates is greater than that of the ordered fibrillar aggregates.[15] Previously, we had proposed that simultaneous His 13-His 14 coordination (subcomponent IC) might be the genesis of this effect. Simultaneous coordination of His 13 and His 14 to Cu(II) is expected to prevent the formation of ordered β-sheet structures, as the side chains of the histidine residues would be forced to be on the same side. In the presence of Zn(II), the proportion of subcomponent IC increases. It has also been postulated that a salt bridge between His 13 and Asp 23 is important for the formation of a key intermediate toward the formation of ordered fibrils.[60,61] Zn(II) or Cu(II) coordination to His 13, even at very low concentrations, may disrupt the salt bridge, leading to the formation of disordered amorphous aggregates rather than ordered aggregates. We performed AFM imaging to test these hypotheses. In the presence of Zn(II), amyloid-β forms more amorphous aggregates (Supporting Information, Figure S5). These AFM experiments were carried out using Aβ(1−40) (Figure 8), as this variant contains the hydrophobic region

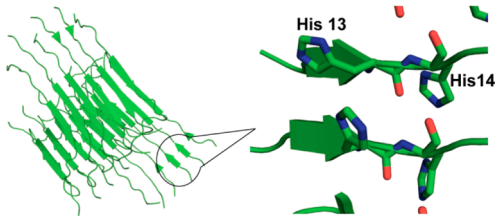

Figure 8. Location of His 13 and His 14 in the fibrillar structure of Aβ(1−40)[59] (PDB code 2LMN).

necessary for aggregation of the peptide, which is absent in Aβ(1−16). In general, when the metal ion concentration increases, the probability of forming fibrillar aggregates decreases. These results suggest that metal ion coordination to His 13 likely plays a decisive role in dictating the morphology of the aggregates. It would be fascinating to directly monitor the disruption of the His 13-Asp 23 salt bridge by solid state NMR.[62]

CONCLUSIONS

We used the well-known metal-binding peptide Aβ, which is involved in Alzheimer's disease, to study the metal-binding competition between Cu(II) and Zn(II). The two metal ions, Cu(II) and Zn(II), have different affinities toward Aβ(1−16), and even at large excess of Zn(II), ~60% of Cu(II) is still bound to Aβ(1−16). Interestingly, Zn(II) was able to replace only Cu(II) coordinated in component I, while component II-bound Cu(II) resisted the Zn(II) substitution. Subcomponent IC in which His 13 and His 14 are equatorially coordinated to a Cu(II) ion becomes the most significant coordination mode. This is a very interesting observation as subcomponent IC might be responsible for the formation of amorphous aggregates. This work shows the ability of ESEEM measuremnts to provide molecular level information of metal ion coordination and competition. Such molecular level details of metal ion coordination may ultimately pave the way to understanding the formation of aggregates of different morphologies and the toxicity associated with Alzheimer's disease.

ASSOCIATED CONTENT

Supporting Information

Proportions of components I and II at different Zn(II) concentrations (Figure S1, Table S1), CW simulations (Figure S2), ESR parameters for CW simulation (Table S2), intensities of the ^{14}N-ESEEM and the ^{1}H-ESEEM region in the three-pulse ESEEM spectra (Table S3, Table S4), HYSCORE spectra (Figure S3), method of calculating subcomponent percentages

dx.doi.org/10.1021/jp406067n | J. Phys. Chem. B 2013, 117, 9386−9394

(Figure S4), and AFM images (Figure S5). This material is available free of charge via the Internet at http://pubs.acs.org.

AUTHOR INFORMATION

Corresponding Author

*E-mail: sksaxena@pitt.edu. Phone: (412) 624-8680. Fax: (412) 624-8611.

Notes

The authors declare no competing financial interest.

ACKNOWLEDGMENTS

This work was supported by a National Institutes of Health grant (5R01NS053788), and a National Science Foundation (MCB 1157712) grant. The Bruker ElexSys E680 was purchased with funds from National Institutes of Health Grant 1S10RR028701. We are grateful to the peptide synthesis facility at the University of Pittsburgh for peptide preparation. We also thank Dr. Byong-kyu Shin and Brian Michael for helpful discussions.

REFERENCES

(1) Maret, W. Metalloproteomics, Metalloproteomes, and the Annotation of Metalloproteins. *Metallomics* **2010**, *2*, 117−125.

(2) Kaplan, J. H.; Lutsenko, S. Copper Transport in Mammalian Cells: Special Care for a Metal with Special Needs. *J. Biol. Chem.* **2009**, *284*, 25461−25465.

(3) Turski, M. L.; Thiele, D. J. New Roles for Copper Metabolism in Cell Proliferation, Signaling, and Disease. *J. Biol. Chem.* **2009**, *284*, 717−721.

(4) Kim, B. E.; Nevitt, T.; Thiele, D. J. Mechanisms for Copper Acquisition, Distribution and Regulation. *Nat. Chem. Biol.* **2008**, *4*, 176−185.

(5) Ducea, J. A.; Bush, A. I. Biological Metals and Alzheimer's Disease: Implications for Therapeutics and Diagnostics. *Prog. Neurobiol.* **2010**, *92*, 1−18.

(6) Blennow, K.; de Leon, M. J.; Zetterberg, H. Alzheimer's Disease. *Lancet* **2006**, *368*, 387−403.

(7) Mattson, M. P. Pathways towards and away from Alzheimer's Disease. *Nature* **2004**, *430*, 631−639.

(8) McKhann, G. M.; Knopman, D. S.; Chertkow, H.; Hyman, B. T.; Jack, C. R., Jr.; Kawas, C. H.; Klunk, W. E.; Koroshetz, W. J.; Manly, J. J.; Mayeux, R.; Mohs, R. C.; Morris, J. C.; Rossor, M. N.; et al. The Diagnosis of Dementia Due to Alzheimer's Disease: Recommendations from the National Institute on Aging-Alzheimer's Association Workgroups on Diagnostic Guidelines for Alzheimer's Disease. *Alzheimer's Dementia* **2011**, *7*, 263−269.

(9) Lovell, M. A.; Robertson, J. D.; Teesdale, W. J.; Campbell, J. L.; Markesbery, W. R. Copper, Iron and Zinc in Alzheimer's Disease Senile Plaques. *J. Neurol. Sci.* **1998**, *158*, 47−52.

(10) Faller, P.; Hureau, C. Bioinorganic Chemistry of Copper and Zinc Ions Coordinated to Amyloid-β Peptide. *Dalton Trans.* **2009**, 1080−1094.

(11) Kepp, K. P. Bioinorganic Chemistry of Alzheimer's Disease. *Chem. Rev.* **2012**, *112*, 5193−5239.

(12) Hureaua, C.; Dorlet, P. Coordination of Redox Active Metal Ions to the Amyloid Precursor Protein and to Amyloid-β Peptides Involved in Alzheimer Disease. Part 2: Dependence of Cu(II) Binding Sites with Aβ Sequences. *Coord. Chem. Rev.* **2012**, *256*, 2175−2187.

(13) Morante, S. The Role of Metals in β-Amyloid Peptide Aggregation: X-Ray Spectroscopy and Numerical Simulations. *Curr. Alzheimer Res.* **2008**, *5*, 508−524.

(14) Viles, J. H. Metal Ions and Amyloid Fiber Formation in Neurodegenerative Diseases. Copper, Zinc and Iron in Alzheimer's, Parkinson's and Prion Diseases. *Coord. Chem. Rev.* **2012**, *256*, 2271−2284.

(15) Jun, S.; Gillespie, J. R.; Shin, B. K.; Saxena, S. The Second Cu(II)-Binding Site in a Proton-Rich Environment Interferes with the Aggregation of Amyloid-β(1−40) into Amyloid Fibrils. *Biochemistry* **2009**, *48*, 10724−10732.

(16) Noy, D.; Solomonov, I.; Sinkevich, O.; Arad, T.; Kjaer, K.; Sagi, I. Zinc-Amyloid β Interactions on a Millisecond Time-Scale Stabilize Non-Fibrillar Alzheimer-Related Species. *J. Am. Chem. Soc.* **2008**, *130*, 1376−1383.

(17) Garai, K.; Sahoo, B.; Kaushalya, S. K.; Desai, R.; Maiti, S. Zinc Lowers Amyloid-β Toxicity by Selectively Precipitating Aggregation Intermediates. *Biochemistry* **2007**, *46*, 10655−10663.

(18) Hamley, I. W. The Amyloid Beta Peptide: A Chemist's Perspective. Role in Alzheimer's and Fibrillization. *Chem. Rev.* **2012**, *112*, 5147−5192.

(19) Damante, C. A.; Ösz, K.; Nagy, Z.; Pappalardo, G.; Grasso, G.; Impellizzeri, G.; Rizzarelli, E.; Sóvágó, I. Metal Loading Capacity of Aβ N-Terminus: A Combined Potentiometric and Spectroscopic Study of Zinc(II) Complexes with Aβ(1−16), Its Short or Mutated Peptide Fragments and Its Polyethylene Glycol−ylated Analogue. *Inorg. Chem.* **2009**, *48*, 10405−10415.

(20) Karr, J. W.; Kaupp, L. J.; Szalai, V. A. Amyloid-β Binds Cu^{2+} in a Mononuclear Metal Ion Binding Site. *J. Am. Chem. Soc.* **2004**, *126*, 13534−13538.

(21) Karr, J. W.; Akintoye, H.; Kaupp, L. J.; Szalai, V. A. N-Terminal Deletions Modify the Cu^{2+} Binding Site in Amyloid-β. *Biochemistry* **2005**, *44*, 5478−5487.

(22) Karr, J. W.; Szalai, V. A. Cu(II) Binding to Monomeric, Oligomeric, and Fibrillar Forms of the Alzheimer's Disease Amyloid-β Peptide. *Biochemistry* **2008**, *47*, 5006−5016.

(23) Syme, C. D.; Nadal, R. C.; Rigby, S. E. J.; Viles, J. H. Copper Binding to the Amyloid-β (Aβ) Peptide Associated with Alzheimer's Disease. *J. Biol. Chem.* **2004**, *279*, 18169−18177.

(24) Drew, S. C.; Noble, C. J.; Masters, C. L.; Hanson, G. R.; Barnham, K. J. Pleomorphic Copper Coordination by Alzheimer's Disease Amyloid-β Peptide. *J. Am. Chem. Soc.* **2009**, *131*, 1195−1207.

(25) Dorlet, P.; Gambarelli, S.; Faller, P.; Hureau, C. Pulse EPR Spectroscopy Reveals the Coordination Sphere of Copper(II) Ions in the 1−16 Amyloid-β Peptide: A Key Role of the First Two N-Terminus Residues. *Angew. Chem., Int. Ed.* **2009**, *48*, 9273−9276.

(26) Shin, B.-k.; Saxena, S. Substantial Contribution of the Two Imidazole Rings of the His13−His14 Dyad to Cu(II) Binding in Amyloid-β(1−16) at Physiological pH and Its Significance. *J. Phys. Chem. A* **2011**, *115*, 9590−9602.

(27) Shin, B.-k.; Saxena, S. Direct Evidence That All Three Histidine Residues Coordinate to Cu(II) in Amyloid-β 1−16. *Biochemistry* **2008**, *47*, 9117−9123.

(28) Gunderson, W. A.; Hernández-Guzmán, J.; Karr, J. W.; Sun, L.; Szalai, V. A.; Warncke, K. Local Structure and Global Patterning of Cu^{2+} Binding in Fibrillar Amyloid-β [Aβ(1−40)] Protein. *J. Am. Chem. Soc.* **2012**, *134*, 18330−18337.

(29) Minicozzi, V.; Stellato, F.; Comai, M.; Serra, M. D.; Potrich, C.; Meyer-Klaucke, W.; Morante, S. Identifying the Minimal Copper- and Zinc-Binding Site Sequence in Amyloid-β Peptides. *J. Biol. Chem.* **2008**, *283*, 10784−10792.

(30) Kozin, S. A.; Zirah, S.; Rebuffat, S.; Hoa, G. H. B.; Debey, P. Zinc Binding to Alzheimer's Aβ(1−16) Peptide Results in Stable Soluble Complex. *Biochem. Biophys. Res. Commun.* **2001**, *285*, 959−964.

(31) Zirah, S. V.; Kozin, S. A.; Mazur, A. K.; Blond, A.; Cheminant, M.; Ségalas-Milazzo, I.; Debey, P.; Rebuffat, S. Structural Changes of Region 1-16 of the Alzheimer's Disease Amyloid β-Peptide upon Zinc Binding and in Vitro Aging. *J. Biol. Chem.* **2006**, *281*, 2151−2161.

(32) Syme, C. D.; Viles, J. H. Solution ^{1}H NMR Investigation of Zn^{2+} and Cd^{2+} Binding to Amyloid-Beta Peptide (Aβ) of Alzheimer's Disease. *Biochem. Biophys. Res. Commun.* **2006**, *1764*, 246−256.

(33) Danielsson, J.; Pierattelli, R.; Banci, L.; Gräslund, A. High-Resolution NMR Studies of the Zinc-Binding Site of the Alzheimer's Amyloid Beta-Peptide. *FEBS J.* **2007**, *274*, 46−59.

(34) Tsvetkov, P. O.; Kulikova, A. A.; Golovin, A. V.; Tkachev, Y. V.; Archakov, A. I.; Kozin, S. A.; Makarov, A. A. Minimal Zn^{2+} Binding Site of Amyloid-β. *Biophys. J.* **2010**, *99*, L84−L86.
(35) Merrifield, R. B. Solid Phase Peptide Synthesis. I. The Synthesis of a Tetrapeptide. *J. Am. Chem. Soc.* **1963**, *85* (14), 2149−2154.
(36) Fields, G. B.; Noble, R. L. Solid Phase Peptide Synthesis Utilizing 9-Fluorenylmethoxycarbonyl Amino Acids. *Int. J. Pept. Protein Res.* **1990**, *35*, 161−214.
(37) Fauth, J. M.; Schweiger, A.; Braunschweiler, L.; Forrer, J.; Ernst, R. R. Elimination of Unwanted Echoes and Reduction of Dead Time in Three-Pulse Electron Spin-Echo Spectroscopy. *J. Magn. Reson.* **1986**, *66*, 74−85.
(38) Gemperle, C.; Aebli, G.; Schweiger, A.; Ernst, R. R. Phase Cycling in Pulse EPR. *J. Magn. Reson.* **1990**, *88*, 241−256.
(39) McCracken, J.; Peisach, J.; Dooley, D. M. Cu(II) Coordination Chemistry of Amine Oxidases. Pulsed EPR Studies of Histidine Imidazole, Water, and Exogenous Ligand Coordination. *J. Am. Chem. Soc.* **1987**, *109*, 4064−4072.
(40) McCracken, J.; Pember, S.; Benkovic, S. J.; Villafranca, J. J.; Miller, R. J.; Peisach, J. Electron Spin-Echo Studies of the Copper Binding Site in Phenylalanine Hydroxylase from *Chromobacterium violaceum*. *J. Am. Chem. Soc.* **1988**, *110*, 1069−1074.
(41) McCracken, J.; Desai, P. R.; Papadopoulos, N. J.; Villafranca, J. J.; Peisach, J. Electron Spin-Echo Studies of the Copper(II) Binding Sites in Dopamine β-Hydroxylase. *Biochemistry* **1988**, *27*, 4133−4137.
(42) Jiang, F.; McCracken, J.; Peisach, J. Nuclear Quadrupole Interactions in Copper(II)-Diethylenetriamine-Substituted Imidazole Complexes and in Copper(II) Proteins. *J. Am. Chem. Soc.* **1990**, *112*, 9035−9044.
(43) McCracken, J.; Peisach, J.; Cote, C. E.; McGuirl, M. A.; Dooley, D. M. Pulsed EPR Studies of the Semiquinone State of Copper-Containing Amine Oxidases. *J. Am. Chem. Soc.* **1992**, *114*, 3715−3720.
(44) Flanagan, H. L.; Singel, D. J. Analysis of Nitrogen-14 ESEEM Patterns of Randomly Oriented Solids. *J. Chem. Phys.* **1987**, *87*, 5606−5616.
(45) Mims, W. B. Envelope Modulation in Spin-Echo Experiments. *Phys. Rev. B* **1972**, *5*, 2409−2419.
(46) Lai, A.; Flanagan, H. L.; Singel, D. J. Multifrequency Electron Spin Echo Envelope Modulation in S=1/2, I=1/2 Systems: Analysis of the Spectral Amplitudes, Line Shapes, and Linewidths. *J. Chem. Phys.* **1988**, *89*, 7161−7166.
(47) Tang, X. S.; Diner, B. A.; Larsen, B. S.; Gilchrist, M. L., Jr.; Lorigan, G. A.; Britt, R. D. Identification of Histidine at the Catalytic Site of the Photosynthetic Oxygen-Evolving Complex. *Proc. Natl. Acad. Sci. U.S.A.* **1994**, *91*, 704−708.
(48) Singh, V.; Zhu, Z.; Davidson, V. L.; McCracken, J. Characterization of the Tryptophan Tryptophyl-Semiquinone Catalytic Intermediate of Methylamine Dehydrogenase by Electron Spin-Echo Envelope Modulation Spectroscopy. *J. Am. Chem. Soc.* **2000**, *122*, 931−938.
(49) Stoll, S.; Calle, C.; Mitrikas, G.; Schweiger, A. Peak Suppression in ESEEM Spectra of Multinuclear Spin Systems. *J. Magn. Reson.* **2005**, *177*, 93−101.
(50) Peisach, J.; Blumberg, W. E. Structural Implications Derived from the Analysis of EPR Spectra of Natural and Artificial Copper Proteins. *Arch. Biochem. Biophys.* **1974**, *165*, 691−708.
(51) Burns, C. S.; Aronoff-Spencer, E.; Dunham, C. M.; Lario, P.; Avdievich, N. I.; Antholine, W. E.; Olmstead, M. M.; Vrielink, A.; Gerfen, G. J.; Peisach, J.; Scott, W. G.; et al. Molecular Features of the Copper Binding Sites in the Octarepeat Domain of the Prion Protein. *Biochemistry* **2002**, *41*, 3991−4001.
(52) Deligiannakis, Y.; Louloudi, M.; Hadjiliadis, N. Electron Spin Echo Envelope Modulation (ESEEM) Spectroscopy as a Tool to Investigate the Coordination Environment of Metal Centers. *Coord. Chem. Rev.* **2000**, *204*, 1−112.
(53) Walter, E. D.; Stevens, D. J.; Visconte, M. P.; Millhauser, G. L. The Prion Protein Is a Combined Zinc and Copper Binding Protein: Zn^{2+} Alters the Distribution of Cu^{2+} Coordination Modes. *J. Am. Chem. Soc.* **2007**, *129*, 15440−15441.
(54) Stellato, F.; Spevacek, A.; Proux, O.; Minicozzi, V.; Millhauser, G.; Morante, S. Zinc Modulates Copper Coordination Mode in Prion Protein Octa-Repeat Subdomains. *Eur. Biophys. J.* **2011**, *40*, 1259−1270.
(55) Damante, C. A.; Ösz, K.; Nagy, Z. N.; Grasso, G.; Pappalardo, G.; Rizzarelli, E.; Sóvágó, I. Zn^{2+}'s Ability to Alter the Distribution of Cu^{2+} among the Available Binding Sites of Aβ(1−16)-Polyethylenglycol-ylated Peptide: Implications in Alzheimer's Disease. *Inorg. Chem.* **2011**, *50*, 5342−5350.
(56) Braymer, J. J.; Choi, J.-S.; DeToma, A. S.; Wang, C.; Nam, K.; Kampf, J. W.; Ramamoorthy, A.; Lim, M. H. Development of Bifunctional Stilbene Derivatives for Targeting and Modulating Metal-Amyloid-β Species. *Inorg. Chem.* **2011**, *50*, 10724−10734.
(57) Jones, M. R.; Service, E. L.; Thompson, J. R.; Wang, M. C. P.; Kimsey, I. J.; DeToma, A. S.; Ramamoorthy, A.; Lim, M. H.; Storr, T. Dual-Function Triazole−Pyridine Derivatives as Inhibitors of Metal-Induced Amyloid-β Aggregation. *Metallomics* **2012**, *4*, 910−920.
(58) Collin, F.; Sasaki, I.; Eury, H.; Faller, P.; Hureau, C. Pt(II) Compounds Interplay with Cu(II) and Zn(II) Coordination to the Amyloid-β Peptide Has Metal Specific Consequences on Deleterious Processes Associated to Alzheimer's Disease. *Chem. Commun.* **2013**, *49*, 2130−2132.
(59) Petkova, A. T.; Yau, W.-M.; Tycko, R. Experimental Constraints on Quaternary Structure in Alzheimer's β-Amyloid Fibrils. *Biochemistry* **2006**, *45*, 498−512.
(60) Kirkitadze, M. D.; Condron, M. M.; Teplow, D. B. Identification and Characterization of Key Kinetic Intermediates in Amyloid Beta-Protein Fibrillogenesis. *J. Mol. Biol.* **2001**, *312*, 1103−1119.
(61) Fraser, P. E.; Nguyen, J. T.; Surewicz, W. K.; Kirschner, D. A. pH-Dependent Structural Transitions of Alzheimer Amyloid Peptides. *Biophys. J.* **1991**, *60*, 1190−1201.
(62) Mithu, V. S.; Sarkar, B.; Bhowmik, D.; Chandrakesan, M.; Maiti, S.; Madhu, P. K. Zn^{+2} Binding Disrupts the Asp^{23}-Lys^{28} Salt Bridge without Altering the Hairpin-Shaped Cross-β Structure of Aβ_{42} Amyloid Aggregates. *Biophys. J.* **2011**, *101*, 2825−2832.
(63) Alies, B.; Sasaki, I.; Sayen, S.; Guillon, E.; Faller, P.; Hureau, C. Zn Impacts Cu Coordination to Amyloid-β, the Alzheimer's Peptide, but Not the ROS Production and the Associated Cell Toxicity. *Chem. Commun.* **2013**, *49*, 2130−2132.

NOTE ADDED IN PROOF

We came across a recent article during the proof stage that indicates Zn(II) ions shift Cu(II) coordination toward component II in this peptide.[63]